Direct measurement of auger recombination in $In_{0.1}Ga_{0.9}N/GaN$ quantum wells and its impact on the efficiency of $In_{0.1}Ga_{0.9}N/GaN$ multiple quantum well light emitting diodes

M. Zhang,[a] P. Bhattacharya,[b] J. Singh, and J. Hinckley
Department of Electrical Engineering and Computer Science, Solid-State Electronics Laboratory, University of Michigan, Ann Arbor, Michigan 48109-2122, USA

(Received 5 August 2009; accepted 26 October 2009; published online 18 November 2009)

The Auger recombination coefficient in $In_{0.1}Ga_{0.9}N/GaN$ quantum wells, emitting at 407 nm has been determined from large signal modulation measurements on lasers in which these quantum wells form the gain region. A value of 1.5×10^{-30} $cm^6\ s^{-1}$ is determined for the Auger coefficient at room temperature, which is used to analyze the reported efficiency characteristics of 410 nm $In_{0.1}Ga_{0.9}N/GaN$ quantum wells light emitting diodes. The calculated efficiencies agree remarkably well with the measured ones. It is apparent that Auger recombination is largely responsible for limiting device efficiencies at high injection currents. © *2009 American Institute of Physics*. [doi:10.1063/1.3266520]

It is recognized that the external quantum efficiency (EQE) of InGaN/GaN (0001) quantum well (QW) light emitting diodes (LEDs) peaks at very low current densities ($\sim$10 A/cm^2) (Ref. 1) and then decreases rather drastically. This trend, which is counter to the requirements for a large number of GaN-based LED applications, has been attributed to several mechanisms[2–4] including nonradiative Auger recombination. In order to ascertain the role of Auger recombination in the operation of these visible light sources, it is first necessary to accurately know the value of the Auger recombination rates. There is only one report on the measurement of Auger recombination in 100–770 Å InGaN single layers grown on sapphire substrates by metal-organic chemical vapor deposition.[5] Large-signal modulation measurements have been utilized to extract the Auger coefficient from InGaAsP/InP QW (Ref. 6) and $In_{0.4}Ga_{0.6}As/GaAs$ quantum dot lasers.[7] We report here the determination of Auger recombination in InGaN/GaN QWs by applying this technique on QW lasers grown on GaN:Si templates. The measured value of the Auger coefficient $C_a=1.5\times10^{-30}$ $cm^6\ s^{-1}$ at 300 K was used to analyze the measured efficiencies[8] of near-UV InGaN/GaN QW LEDs. The calculated efficiencies, using our measured value of the Auger coefficient, agree remarkably well with the measured ones. It is apparent that Auger recombination is a major contributor to the observed "efficiency droop" of InGaN/GaN QW LEDs.

The QW laser heterostructure is shown in Fig. 1(a). The device tested has an area of 4×390 μm^2. The measured light-current (*L-I*) characteristics of the laser with cw current injection are shown in Fig. 1(b). The output spectral characteristics, measured with a spectrometer having a resolution of 0.35 nm are shown in the inset to Fig. 1(b). The peak emission is at 407 nm and the linewidth of the emission is $\sim$1 nm at an injection current of 90 mA. The threshold current $I_{th}=30$ mA.

The basis for the determination of the Auger coefficients is the carrier rate equation below threshold

$$\frac{dn}{dt}=\frac{I}{qV}-R(n), \tag{1}$$

where I is the injection current, V is the active region volume, and the total recombination rate $R(n)$ is expressed as

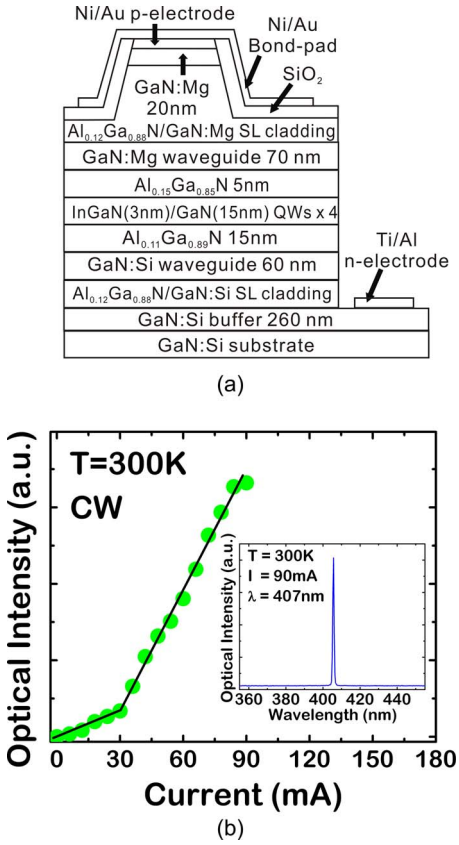

FIG. 1. (Color online) (a) Schematic of InGaN/GaN MQW laser heterostructure grown on (0001)-GaN:Si substrate and (b) measured light-current characteristics of the laser. Inset shows the output spectral characteristics of the laser.

[a]Electronic mail: mezhang@umich.edu.
[b]Electronic mail: pkb@eecs.umich.edu.

$$R(n) = \frac{n}{\tau} = A_{\mathrm{nr}} n + R_{\mathrm{sp}} n^2 + C_a n^3, \tag{2}$$

in terms of the carrier lifetime τ, the carrier density n, the Shockley–Read–Hall (SRH) coefficient A_{nr}, the radiative recombination coefficient R_{sp}, and the Auger recombination coefficient C_a. Integration of Eq. (1) with appropriate boundary values yields the expression for the turn-on delay time

$$\tau_d = qV \int_0^{n_{\mathrm{th}}} \frac{1}{I - qVR(n)} dn. \tag{3}$$

Therefore measurement of the stimulated emission delay times, calculation of the radiative recombination rates, and the SRH recombination rates allow an accurate determination of the threshold carrier density and the Auger coefficient in a self-consistent manner. n_{th} is related to the threshold current density J_{th} by

$$J_{\mathrm{th}} = qdR(n_{\mathrm{th}}) = qd(A_{\mathrm{nr}} n_{\mathrm{th}} + R_{\mathrm{sp}} n_{\mathrm{th}}^2 + C_a n_{\mathrm{th}}^3). \tag{4}$$

where d is the effective thickness of the recombination region.

In the large-signal modulation measurement technique, the laser diode is driven by 120 ns current pulses (15% duty cycle) with 100 ps rise time (20%–80%) switching from $I=0$ to $I\,[>I_{\mathrm{th}}$—see Fig. 1(b)]. An impedance matching unit is used to reduce the distortion of the driven pulses. The light output is collected by a 50× objective lens and coupled into an ultrahigh-speed GaAs photodetector via a short single mode optical fiber and temporally resolved with a 10 GSa/s sampling oscilloscope. The electrical bias pulse is concurrently fed into the scope. Typical results are shown in Fig. 2(a), from which it can be seen that there is a turn-on delay between the electrical bias pulse and the laser output, taking into account the delays in the rf cable, optical fiber, and detector (accurate to ±40 ps). The delay time decreases from 2.70 to 0.51 ns with increasing current [Fig. 2(b)], as higher current density leads to a shorter recombination lifetime and consequently the delay time.

In order to determine the Auger coefficient accurately using Eqs. (2)–(4), it is important to have accurate values of the coefficients A_{nr} and R_{sp}. Assuming high current injection conditions and that the electron density is equal to the hole density ($n=p \gg n_i$), the value of A_{nr} is estimated as follows: $A_{\mathrm{nr}} \cong \sigma v_{\mathrm{th}} N_t/2$, where σ is the capture cross section of the deep level, v_{th} is the thermal velocity, and N_t is the deep level density. The values of σ and N_t were extracted from deep level transient spectroscopy measurements on the near-UV laser. Two distinct deep levels, labeled L_1 and L_2, were observed. Their activation energies E_t are 0.2 and 0.6 eV (measured from the conduction band edge) and capture cross-section σ are 9.0×10^{-16} and 4.8×10^{-15} cm^2, respectively. The total trap concentration $N_T \sim 2\times10^{14}$ cm^{-3}. A value of $A_{\mathrm{nr}}=1\times10^7$ s^{-1} is obtained with these parameter values and used in this study. By using a well developed nitride device simulator at the University of Michigan, the value of R_{sp} is calculated using Fermi's golden rule with an eight-band $\mathbf{k}\cdot\mathbf{p}$ description of the bands. A value of 2×10^{-11} cm^3 s^{-1} is obtained, taking into account the polarization field and interface strain in the active region. This value is very close to the value of R_{sp} reported by Bulashevich *et al.*[9] (2.4×10^{-11} cm^3 s^{-1}). The value of C_a and n_{th} were determined iteratively by using Eqs. (3) and (4) in a self-consistent manner, for the different injection currents, with the measured delay times τ_d. The threshold carrier density (n_{th}) is calculated to be 1.52×10^{19} cm^{-3}. A value of $C_a=1.5\times10^{-30}$ cm^6 s^{-1} at 300 K is obtained, which compares favorably with values of $(1.4–2.0)\times10^{-30}$ cm^6 s^{-1} measured in $\mathrm{In}_x\mathrm{Ga}_{1-x}N(0.09\leq x\leq 0.15)$ single layers.[5]

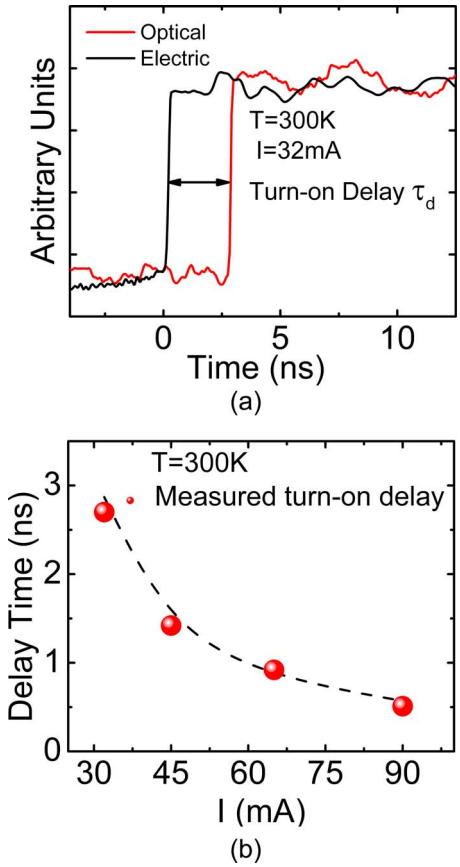

FIG. 2. (Color online) (a) Measured turn-on delay between the electrical large-signal bias the coherent optical signal from the laser and (b) measured variation of turn-on delay times with injection current.

The values of the EQE of 410 nm InGaN/GaN LEDs reported by Yang *et al.*[8] were analyzed using the measured value of C_a quoted above. The internal quantum efficiency (IQE) of the LEDs is expressed as

$$\eta_{\mathrm{int}} = \frac{R_{\mathrm{sp}} n^2}{R(n)} = \frac{R_{\mathrm{sp}} n^2}{A_{\mathrm{nr}} n + R_{\mathrm{sp}} n^2 + C_a n^3}. \tag{5}$$

In order to plot η_{int} as a function of current density J, instead of n, Eq. (4) is used for the conversion between n and J. Since the band offset between the $\mathrm{In}_{0.1}\mathrm{Ga}_{0.9}N$ wells and GaN barriers in the near-UV LEDs is relatively small, it is assumed that transport of injected holes is not obstructed by the barriers and the diffusion length of the holes is long enough,[10] such that they are injected uniformly into all the wells. Since nearly all the carriers recombine in the QW region, the effective recombination thickness d is taken to be 12 nm. The calculated plot relating n and J is shown in the inset of Fig. 3(a). Calculated values of IQE (η_{int}) as a function of J are depicted by the solid curve in Fig. 3(a). The peak IQE is calculated to be 70% (at a current density of 40 A/cm^2), which is typically measured for near-UV InGaN/GaN QWs.[11] The measured variation of EQE (η_{exe}) reported by Yang *et al.*[8] is also shown in the same figure by

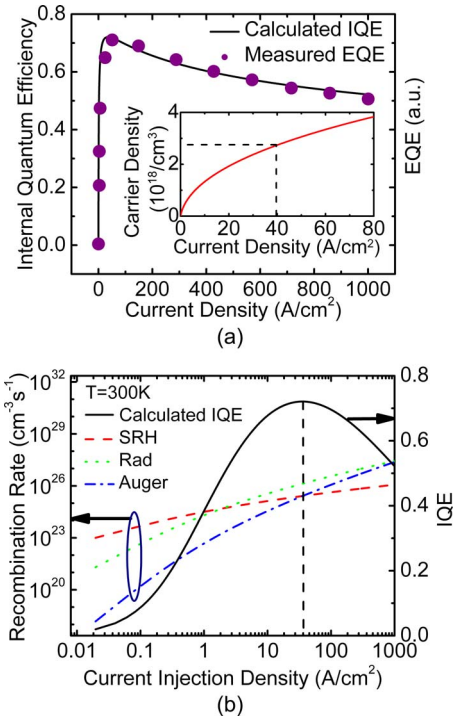

FIG. 3. (Color online) (a) Calculated IQE (solid line) as a function of injection current of near-UV InGaN/GaN QW LED. The inset shows the calculated relation between the carrier density in the QWs and the current density. The dashed lines signify the point of maximum efficiency. The solid circles indicate reported data (Ref. 6) for a LED emitting at nearly the same wavelength and (b) calculated SRH (dashed line), radiative (dotted line), and Auger (dash-dotted line) recombination rates as a function of injection current density. The crossover of the SRH and Auger recombination rates corresponds to the maximum IQE.

the closed circles. It should be noted that a scaling factor has been used to match the two efficiencies. This factor is essentially the extraction efficiency $\eta_{\text{extraction}}$ due to total internal reflection inside the LED heterostructure. Thus $\eta_{\text{int}}(J) = \eta_{\text{extraction}} \times \eta_{\text{ext}}(J)$. The important point to note is that the *trend* of the two efficiencies agree with each other remarkably well. The calculated variation of Auger, radiative, and SRH recombination rates with injected current density are illustrated in Fig. 3(b). It is evident that Auger recombination dominates for $J \geq 40$ A/cm^2($n \cong 2.75 \times 10^{18}$ cm^{-3}). The onset of the reduction in LED efficiency also occurs at this current density. It should be noted that in the data reported by Yang *et al.*,[8] the EQE is strongly dependent on the duty cycle of the pulsed current injection, particularly at high current densities. The comparison made in Fig. 3(a) is for a reported duty cycle of 0.1%, for which heating effects are minimized.

It is of interest to note that the measured value of C_a in the InGaN/GaN near-UV QWs is lower than those measured for the InGaAs/InP QWs ($\sim 10^{-29}$ cm^6 s^{-1}), where a reduction in efficiency is not observed at similar levels of injection current.[12,13] However, the carrier density in the InGaN wells is much larger than that in the InGaAs wells for the same injection, because the carrier density ($n \sim J\tau/d$) depends not only on the current density (J) but also on the QW thickness (d) and the carrier lifetime (τ). Therefore, in comparing arsenide and nitride devices at the same current injection (J), the effect of recombination time and well thickness on n must be considered. In arsenide devices, τ is characteristically smaller than in nitride devices and d is generally larger. The reasons why τ is larger in nitride QWs are (1) the carrier thermal velocity (mobility) is smaller in nitride wells, since the scattering is strong due to the higher DOS (larger electron effective mass) and (2) the spatial separation between electron and hole is larger in nitride wells because of the internal electrical field. Therefore the Auger recombination rate ($C_a n^3$) is larger in the nitride QWs, although the Auger coefficient is smaller, and plays a dominant role in limiting the efficiency of LEDs. In longer wavelength (blue and green) LEDs, the peaking and reduction in efficiency are observed at smaller current densities (~ 10 A/cm^2). This is due to a larger expected value of C_a in the smaller bandgap $In_{0.2}Ga_{0.8}N$ QWs used, since the Auger coefficient is proportional to $(k_B T/E_g)^{3/2}\exp(-E_g/k_B T)$ (Ref. 14) where E_g is the band gap. Furthermore, the tilted bands due to the higher degree of polarization electric field in the blue-green emission QWs (~ 1.7 MV/cm) will further increase the carrier density in the wells.[15]

The work is supported by the Department of Energy under Grant No. DEFC2607NT43229.

[1]T. Mukai, M. Yamada, and S. Nakamura, Jpn. J. Appl. Phys., Part 1 **38**, 3976 (1999).
[2]B. Monemar and B. E. Sernelius, Appl. Phys. Lett. **91**, 181103 (2007).
[3]M. H. Kim, M. F. Schubert, Q. Dai, J. K. Kim, E. F. Schubert, J. Piprek, and Y. Park, Appl. Phys. Lett. **91**, 183507 (2007).
[4]N. F. Gardner, G. O. Müller, Y. C. Shen, G. Chen, S. Watanabe, W. Götz, and M. R. Krames, Appl. Phys. Lett. **91**, 243506 (2007).
[5]Y. C. Shen, G. O. Mueller, S. Watanabe, N. F. Gardner, A. Munkholm, and M. R. Krames, Appl. Phys. Lett. **91**, 141101 (2007).
[6]H. Yoon, A. L. Gutierrez-Aitken, R. Jambunathan, J. Singh, and P. Bhattacharya, IEEE Photon. Technol. Lett. **7**, 974 (1995).
[7]S. Ghosh, P. Bhattacharya, E. Stoner, J. Singh, H. Jiang, S. Nuttinck, and J. Laskar, Appl. Phys. Lett. **79**, 722 (2001).
[8]Y. Yang, X. A. Cao, and C. Yan, IEEE Trans. Electron Devices **55**, 1771 (2008).
[9]K. A. Bulashevich, V. F. Mymrin, S. Y. Karpov, I. A. Zhmakin, and A. I. Zhmakin, J. Comput. Phys. **213**, 214 (2006).
[10]K. Kumakura, T. Makimoto, N. Kobayashi, T. Hashizume, T. Fukui, and H. Hasegawa, Appl. Phys. Lett. **86**, 052105 (2005).
[11]J. M. Phillips, M. E. Coltrin, M. H. Crawford, A. J. Fischer, M. R. Krames, R. Mueller-Mach, G. O. Mueller, Y. Ohno, L. E. S. Rohwer, J. A. Simmons, and J. Y. Tsao, Laser Photonics Rev. **1**, 307 (2007).
[12]L. Davis, Y. Lam, D. Nichols, J. Singh, and P. Bhattacharya, IEEE Photonics Technol. Lett. **5**, 120 (1993).
[13]N. F. Massé, A. R. Adams, and S. J. Sweeney, Appl. Phys. Lett. **90**, 161113 (2007).
[14]P. Bhattacharya, in *Semiconductor Optoelectronic Devices*, edited by P. Hall, 2nd ed. (Prentice Hall, Englewood Cliffs, NJ, 1996).
[15]M. Zhang, J. Moore, Z. Mi, and P. Bhattacharya, J. Cryst. Growth **311**, 2069 (2009).